Two-step yielding and directional strain-induced strengthening in dilute colloidal gels

Hubert K. Chan and Ali Mohraz*
Department of Chemical Engineering & Materials Science, University of California, Irvine, California, USA
(Received 1 February 2012; published 16 April 2012)

We investigate the nonlinear rheology of dilute, depletion-induced colloidal gels and report that these systems yield via a two-step process. We propose the two yield points to be associated with interparticle bond rotation and bond breakage, respectively. These distinct yielding mechanisms lead to remarkable creep profiles at intermediate values of the applied stress, highlighted by an anisotropic shear-induced strengthening and flow arrest at very large accumulated strains ($\gamma \sim 80$). The possible microstructural origins of this behavior are discussed.

DOI: 10.1103/PhysRevE.85.041403 PACS number(s): 82.70.Dd, 82.70.Gg, 83.50.−v

I. INTRODUCTION

Attractive interparticle interactions can induce a transition in colloidal dispersions from a fluidlike suspension to a gel, which is characterized by the formation of a dynamically arrested, sample-spanning particle network. This transition typically imparts unique and complex rheological properties to these mixtures [1], which have long been exploited for their use in food and personal care products [2], paints [3], filtration membranes [4], and ceramics processing [5] to name a few. Colloidal gels are also promising materials for feedstocks in emerging technologies, including the direct writing of complex three-dimensional structures [6] with uses in microfluidics [7] and photonic materials [8]. Investigation of the convoluted factors that govern the rheology of colloidal gels not only furthers our scientific understanding of the physics of complex and structured fluids, but also paves the way for improvements and extensions to their applications. Previous studies have correlated the salient rheological properties of colloidal gels in the linear (small amplitude strain) regime to particle size [9,10], colloid volume fraction [11,12], gel structure [13], and strength of interparticle attraction [9,14]. In addition, the steady-shear rheology of colloidal gels has been thoroughly characterized [15,16]. However, as gels must often undergo finite deformations beyond their limit of linear viscoelasticity during either processing (e.g., ejection from a printer nozzle in direct writing) or final consumer use (e.g., the application of personal care and cosmetic products), it is sometimes the viscoelastic response to these transient nonlinear (large-strain) deformations that is of practical interest. The nonlinear rheology of colloidal gels also presents challenging questions and unresolved physics due to the two-way coupling between the globally applied stresses and the complex microstructural changes that accompany large-strain deformations in these systems.

Previous reports on the nonlinear rheology of colloidal gels have focused on understanding the mechanisms of yielding and stress relaxation during large-strain deformations [10,17–21]. It has been suggested that the stress-induced transition from solidlike to fluidlike behavior in some dense gels and weakly attractive glasses occurs in two steps, each at a distinct value of the applied stress [19,20,22–25]. The first step is associated with irreversible interparticle bond breakage—at stresses below this first yield point, interparticle links are capable of reversible elastic bending or stretching. Due to the high colloid volume fraction in these systems, particles are also caged by their nearest neighbors [26]. The second yield step, which occurs at a yet higher value of the applied stress and leads to fluidlike behavior, is attributed to cage breaking and a change in the topological neighbors of particles. Between the two yield points, particles are able to change bonding neighbors but retain the same topological neighbors [20,23]. Experimental evidence for two-step yielding has been found from stress-sweep tests that measure the material's elastic (G') and loss (G'') moduli over a range of applied oscillatory stresses. The two yield stresses are generally identified by their corresponding distinct peaks in G'', which represent the energy dissipated by bond and cage breaking, respectively [22]. Typically, the second yield point also coincides with a crossover between G' and G'', representing the transition from solidlike to fluidlike behavior. The separation between bond- and cage-breaking stresses also brings about nontrivial responses to step stress (creep) experiments in which a constant shear stress σ is applied to the sample and the resulting strain γ is recorded as a function of time [20,25,27]. Dense gels that undergo two-step yielding exhibit elastic distortion when σ is below the bond breaking stress, fluidlike flow above the cage-breaking stress, and plastic deformation through local shear transformation zones between the two stresses [20]. It has been suggested that the occurrence of two-step yielding also depends on the colloid volume fraction ϕ; experiments have shown that the second peak in G'' becomes less prominent as ϕ is decreased until it eventually disappears altogether at $\phi \sim 0.2$ [19,24]. Presumably, the caging effect is diminished for $\phi < 0.2$ with a decrease in the number of topological neighbors surrounding each particle. This viewpoint suggests a single-step yielding mechanism for dilute gels ($\phi < 0.2$), which would be associated with interparticle bond breakage. However, in dilute systems with relatively centrosymmetric interparticle potentials and thin cluster backbones (e.g., strong depletion interactions in suspensions of spherical particles), pairwise angular displacements between neighbors may be more freely allowed than bond breakage [28]. Some previous studies have shown experimental support for soft pivot points [29,30], while others have suggested that surface friction may allow interparticle bonds to support a finite torque before significant angular rearrangement [31,32], but note that such pairwise rotation mechanisms are topologically restrained and nearly absent in dense systems. The implications of such soft

*mohraz@uci.edu

pivot points for the yielding and creep behavior of dilute colloidal gels can be significant but have to date remained unexplored.

In this paper, we investigate the nonlinear rheology of dilute ($\phi = 0.05$) density- and refractive index-matched colloidal gels formed by depletion attractions. We present results obtained from oscillatory stress sweeps and step stress experiments, and report that these systems also undergo two-step yielding. We postulate that instead of the bond and cage-breaking mechanisms associated with dense networks, dilute gels first yield via bond rotation and secondly by widespread bond rupture. The observed distinction between bond rotation and rupture points can lead to remarkable creep profiles at intermediate values of the applied stress, highlighted by shear-induced strengthening at large strains ($\gamma > 10$), which dramatically increases the gels resistance to subsequent deformation. We also show that the enhanced resistance only occurs in the original shear direction and discuss the possible microstructural origins of this behavior. Our results reveal phenomena related to the nonlinear rheology of dilute colloidal gels and put forward questions for future research in this area.

II. MATERIALS AND METHODS

Monodisperse, fluorescently labeled polymethylmethacrylate (PMMA) microspheres (diameter ≈ 1.6 μm) with a sterically stabilizing graft layer of polyhydroxystearic acid were synthesized according to previously reported methods [33,34]. Samples were prepared in a mixture of *cis*-decahydronaphthalene (*cis*-D, Chemsampco, Dallas, TX) and cyclohexyl bromide (CHB, Sigma-Aldrich, St. Louis, MO) at a mass ratio of 24.75/75.25. This optimal solvent mixture provides simultaneous density- and refractive-index matching with the PMMA particles, which not only prevents particle sedimentation or creaming, but minimizes the effects of van der Waals interparticle forces. In addition, the use of a model system that is optimized for confocal microscopy will allow the direct comparison of future microstructural studies with our results. To reduce electrostatic interactions between the particles, the CHB solvent was first purified [35]. Attractive depletion interactions were induced by the addition of a nonadsorbing polymer, polystyrene (PS, $M_w = 777\,500$, $M_w/M_n = 1.04$, Sigma-Aldrich). The PMMA particles were uniformly suspended in the CHB/*cis*-D solvent mixture by vortex mixing and bath ultrasonication for approximately 30 s each and allowed to equilibrate for at least 24 h. Separately, stock solutions of the nonadsorbing polymer were prepared by vortex mixing dry PS with CHB/*cis*-D to achieve a concentration $C_p = 50$ mg/mL and given at least 48 h to reach equilibrium. Samples were prepared by combining the necessary amount of PS stock to the colloid suspension to produce a final $\phi = 0.05$ and $C_p = 10$ mg/mL, resulting in an attractive depletion potential of approximate strength $U/kT \sim 103$ at contact [36].

All rheological measurements were performed on a stress-controlled rheometer (MCR301, Anton Paar, Graz, Austria) with cone-and-plate geometry using a sandblasted cone (diameter = 25 mm, 2° angle). A solvent trap chamber was utilized to prevent evaporation. Each sample was transferred to the rheometer as soon as prepared and allowed at least 30 min to quiescently form a gel at the constant measurement temperature of 26 °C. We ensured that this wait period was long enough for G' to reach a constant plateau value [37]. The gel's nonlinear rheological properties were then characterized via a stress sweep test at frequency $f = 1$ Hz, or a step stress experiment over a span of 3 min. If multiple step stress experiments were planned for a sample, a wait period of 1 min was administered between the tests.

III. RESULTS AND DISCUSSION

Figure 1(a) shows the results of an oscillatory stress sweep experiment for a representative sample at $\phi = 0.05$, $C_p = 10$ mg/mL. Solidlike behavior ($G' > G''$) is observed at low values of σ, typical of colloidal gels. Interestingly, there are two distinct peaks in G'' (highlighted by arrows), also coincident with drops in G', indicative of a two-step yielding mechanism. At the first yield point, which produces a broad G'' peak centered near $\sigma_{y1} \approx 0.6$ Pa, G' shows a clear and measurable drop but remains larger than G''. The dilute gel therefore retains a solidlike character after the structural transformations associated with the first yield point, which is reportedly not always the case for dense gels. In dense systems, G' can fall below G'' at stresses below the cage breaking point if the interparticle attraction strength or the colloid volume fraction is sufficiently low [19,20,22,24]. In such cases, the second yield point corresponds to the breakup of already-flowing clusters or cages into individual particles. Clearly, the two-step yielding mechanism of dilute gels seen here cannot be attributed to the same mechanisms as in dense gels. As shown schematically in Fig. 1(b), we propose instead that the energy dissipation peak at σ_{y1} corresponds to the unraveling and reorganization of the tenuous gel backbone via pairwise angular displacements between neighbor pairs. This picture is consistent with previous studies of transient gel deformation during shear startup at constant rate [29,30] and supports the notion of soft pivot points in colloidal

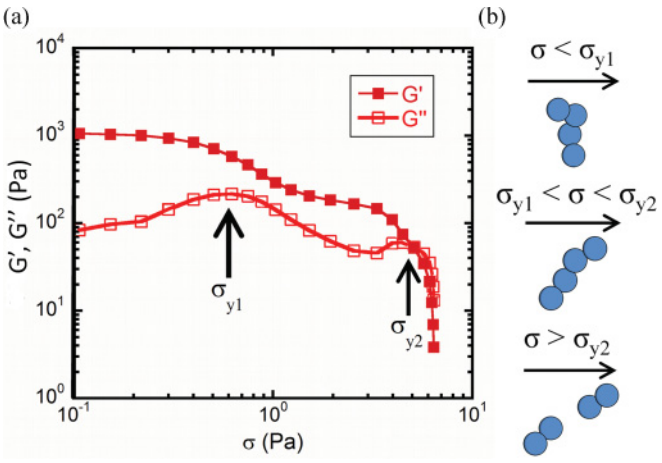

FIG. 1. (Color online) (a) Oscillatory stress sweep at $f = 1$ Hz for a dilute ($\phi = 0.05$) depletion-induced colloidal gel. The arrows highlight the two distinct yield points, corresponding to the peaks in the loss modulus (G'') and simultaneous drops in the storage modulus (G'). (b) Schematic that illustrates the proposed unraveling and eventual rupture of a gel backbone as σ is increased.

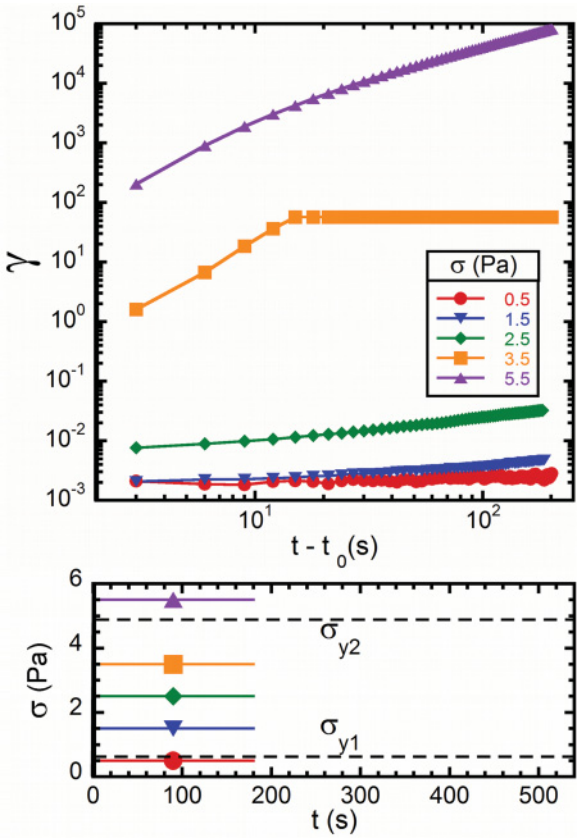

FIG. 2. (Color online) Step stress experiments on quiescent samples for a range of constant applied stresses. The bottom graph shows the stress history in relation to σ_{y1} and σ_{y2}.

gels when the interparticle interactions are centrosymmetric [28]. These studies have suggested that bond rotations allow the microstructure to transition from the isotropic quiescent network to one mostly populated with aligned particle chains in response to a large-strain deformation. In light of these arguments, the transition at σ_{y1} in Fig. 1(a) probably represents the unraveling of the tenuous gel backbone via pairwise angular displacements. The gel, however, retains a solidlike character ($G' > G''$), presumably because the particle network still retains its sample-spanning connectivity. Increasing σ would eventually result in a second yield point ($\sigma_{y2} \approx 5$ Pa), which we attribute to rupture along the gel backbone. With widespread bond breakage, the suspension enters a fluidlike regime, and G' rapidly drops below G''.

We further probed the implications of two-step yielding in dilute gels through step stress measurements at carefully chosen values of the applied stress (Fig. 2). Here t_0 denotes the start time for each test, such that $t - t_0$ is the elapsed time in each experiment. For $\sigma = 0.5$ Pa, which is below σ_{y1}, the creep profile is practically flat at $\gamma \sim 10^{-3}$, which is attributed to elastic deformation in the linear viscoelasticity regime [20,25]. Also expected is the fluidlike behavior at $\sigma = 5.5$ Pa, recognizable by the late-stage linear increase of γ with time, as stresses well above σ_{y2} should result in widespread bond breakage and flow. At intermediate values of σ, we anticipate nontrivial creep behavior due to the interplay between bond rotation and rupture. For values of σ slightly above σ_{y1} ($\sigma = 1.5$ Pa and 2.5 Pa), the dilute gel undergoes gradual but continuous deformation for the entire duration of the experiment, as evident by the sublinear unbounded increase of γ with time. This behavior is consistent with the creep profile of dense particulate suspensions below their cage-breaking yield stress [20,25] and presumably occurs in our system through stress-induced interparticle bond rotations along the gel's tenuous backbone. Strain recovery tests in this range of σ reveal a gradual transition from primarily elastic to plastic deformation in the gel as σ is increased above σ_{y1} [37]. At σ just below σ_{y2} ($\sigma = 3.5$ Pa, onset of the second peak in G''), an intriguing two-stage creep profile is unveiled; the application of stress initially results in significant shear strain, but remarkably, the sample appears to abruptly reach a stress-bearing state, and deformation is completely halted.

The general shape of the $\sigma = 3.5$ Pa profile resembles the initial stages of creep deformation previously reported for a variety of pastes [27] and a presheared thixotropic suspension [38] below their respective yield points. For pastes, the creep profile is initially similar to the deformation of an ideal solid; the accumulated strain plateaus at values of order $\gamma \sim 10^{-2}$ once the applied stress can no longer elastically deform the material. However, continued application of stress eventually leads to slow plastic deformation of the paste. In the thixotropic sample, the initial strain profile corresponds to shear flow in a fluidlike presheared suspension that reaches a strain plateau upon gelation. Our experiments, however, present a fundamentally different scenario from these studies. First, our starting point is a quiescent dilute colloidal gel; our results are therefore not applicable to the presheared fluidlike suspension. Second, the plateau strain in our system ($\gamma \approx 80$) is about 3 orders of magnitude larger than those seen in pastes ($\gamma \sim 10^{-2}$) and represents a different mechanism of shear-induced arrest. Third, in our system, the initial deformation leading to the strain plateau is plastic in nature [37], whereas in pastes it is primarily elastic. Finally, we note that once the plateau regime is reached in our samples, the continued application of stress at $\sigma = 3.5$ Pa results in no further deformation for at least several hours [37]. In contrast, pastes enter a third regime of plastic deformation upon continued application of the stress [27]. Based on these remarks, we propose that the initial deformation at $\sigma = 3.5$ Pa here may be accommodated by the rearrangement of particles into extended chains, similar to the transient microstructures observed in dilute gels during shear startup at a constant nominal rate [30]. Such configurations are realized primarily through bond rotation events, which also govern the first yield point in these materials. However, here the samples achieve exceedingly large values of strain ($\gamma \approx 80$) before reaching a plateau. This observation suggests that occasional bond rupture might have also occurred during the plastic deformation stage. To examine this notion, we estimated the maximum dimensionless strain that could be reached from backbone unraveling alone in our system. We consider the topology of our quiescent gels to be fractal, described by $L \propto h^{d_B}$, where L and h are the chemical length and physical distance between any two points along the cluster backbone, and d_B is the backbone dimension, typically found to be 1.2 for diffusion-limited cluster aggregation [39]. The maximum possible shear strain without bond rupture is achieved when a large cluster spanning the entire gap between the cone edge

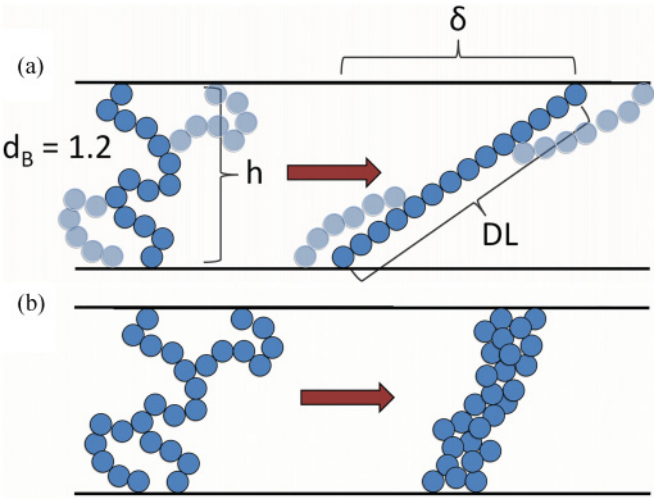

FIG. 3. (Color online) Illustration detailing the proposed microstructural mechanisms for flow arrest. (a) Transition of a fractal cluster (backbone dimension $d_B = 1.2$) into an extensional force chain under shear. Note that this scenario is likely an exaggeration and is intended to present the maximum strain achievable prior to bond rupture. (b) Formation of a stress-bearing gel backbone through shear-induced cluster densification.

and the bottom plate unravels fully into a straight chain, as illustrated in Fig. 3(a). Assuming monodisperse particles with average diameter D, and using the normalized values $H = \frac{h}{D}$ and $\Delta = \frac{\delta}{D}$, we can estimate

$$DL \approx DH^{1.2}, \quad L \approx H^{1.2}.$$

From geometry:

$$H^2 + \Delta^2 = L^2 = (H^{1.2})^2, \quad \gamma = \frac{\Delta}{H} = \sqrt{H^{0.4} - 1}.$$

Using our system geometry (25-mm diameter cone, 2°), we calculate that this maximum strain would be $\gamma \approx 2.9$. Note that this estimated value represents an upper bound since (1) the entire gap is assumed to be a single fractal cluster—in reality, the fractal scaling only applies within a characteristic cluster size that itself depends on ϕ [40]; and (2) the strain is calculated at the cone edge—because of the gel's fractal topology, the largest achievable strain increases with the cluster size [29], and assuming that the entire gap is filled by one cluster, it is maximized at the cone edge. Clearly, the strain plateau for the $\sigma = 3.5$ Pa profile in Fig. 2 is far beyond the calculated upper bound, corroborating that a number of particle chains must have been ruptured during the initial deformation period and before the final stress-bearing configuration is achieved. Given the proximity of σ to σ_{y2} in this case, the proposed local bond breakage scenario is conceivable. Remarkably, the combined rupture and bond rotation events lead to a surprisingly reproducible deformation behavior (compare, for example, the $\sigma = 3.5$ Pa profiles in Figs. 2, 4, and 5, which represent independent experiments).

Previous studies on dilute colloidal gels have reported the occurrence of a stress overshoot at large values of the accumulated strain ($\gamma > 1.5$) during the startup of steady, constant-rate shear flow, which also coincides with the formation of anisotropic structures [29,30,41]. We propose

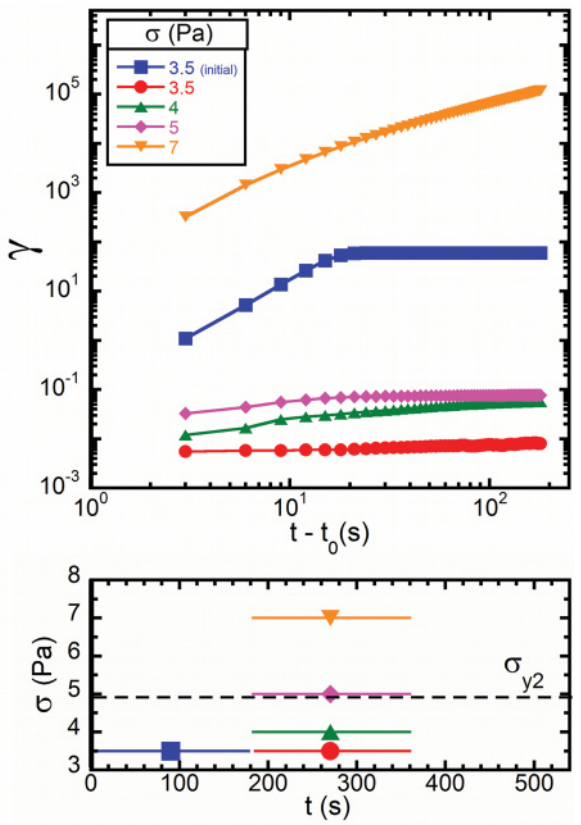

FIG. 4. (Color online) Multiple step stress experiments on a sample illustrating shear-induced gel strengthening. The bottom graph shows the stress history in relation to σ_{y1} and σ_{y2}.

that a similar mechanism may be at play here, and the load-bearing state observed at $\sigma_{y1} < \sigma < \sigma_{y2}$ may be due to the formation of what we consider extensional force chains in the system—almost linear chains of particles oriented near the extensional component of shear flow (45° from the flow direction), as depicted schematically in Fig. 3(a). This fully extended chain would be the most stress-bearing configuration for a cluster of particles containing soft pivot points, and once formed, prevents the microstructure from further deformation unless interparticle bonds are broken. While our speculations about anisotropic structure formation were arrived at based on previous studies described above, we acknowledge that the observed plateau in the accumulated strain may be due to a different microstructural mechanism such as shear-induced cluster densification and the formation of locally favored structures that can lead to dynamic arrest [42,43], as schematically illustrated in Fig. 3(b). Given the large magnitude of γ at its plateau, the cluster densification scenario is particularly plausible. Future flow microscopy studies are therefore warranted to thoroughly understand the microstructural origins of the observed behavior.

To gain further insight into the strain-induced stress-bearing state revealed in Fig. 2, we performed additional experiments on the system after the strain plateau had been reached. The sample was first subjected to $\sigma = 3.5$ Pa and a deformation profile similar to that in Fig. 2 was observed. The applied stress was removed for a wait period of 1 min, and the already-deformed sample was then subjected to repeat step

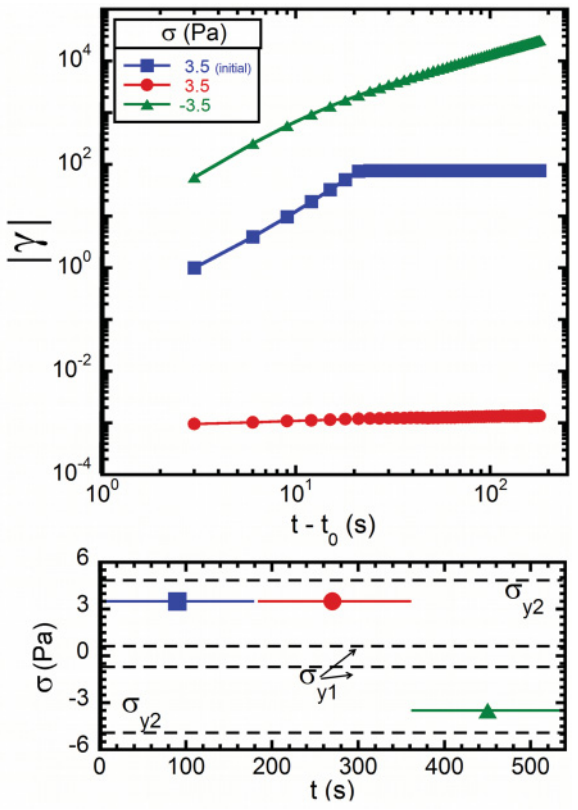

FIG. 5. (Color online) Multiple step stress experiments on a sample illustrating that the shear-induced gel strengthening is asymmetric and only occurs in the original strain direction. The bottom graph shows the stress history in relation to σ_{y1} and σ_{y2}.

stress experiments at different values of σ (Fig. 4). The strain profiles for repeat tests at $\sigma = 3.5$ Pa and 4 Pa are effectively flat, confirming that the gel is now significantly stronger than its quiescent state. As σ approaches σ_{y2} ($\sigma = 5$ Pa), the creep profile becomes qualitatively similar to that of a quiescent gel deformed at a much lower $\sigma = 2.5$ Pa, showing a gradual increase in the accumulated strain. However, we propose that these two processes are governed by fundamentally different mechanisms; the creep deformation of the quiescent gel at σ slightly above σ_{y1} ($\sigma = 2.5$ Pa) primarily occurs through bond rotation and backbone unraveling, whereas for the stress-bearing configuration it is mediated by isolated rupture events at $\sigma \sim \sigma_{y2}$. Finally, $\sigma = 6$ Pa results in fluidlike behavior, which we attribute to widespread rupture at $\sigma > \sigma_{y2}$. These findings unveil an intriguing mechanism of nonlinear strain-induced strengthening in dilute colloidal gels.

To assess whether the enhanced creep resistance is associated with the formation of an anisotropic microstructure in the gel, we studied the effects of stress reversal on shear-strengthened samples (Fig. 5). As before, we first allowed the load-bearing configuration to form by deformation from a quiescent state at $\sigma = 3.5$ Pa. The applied stress was then removed and after a wait period of 1 min, employed again in the forward or reverse direction. Similar to what was seen in Fig. 4, a subsequent test at $\sigma = 3.5$ Pa in the forward direction produces a flat strain profile, indicative of a fully immobilized structure. But when the stress direction is reversed, the sample immediately begins to deform in the opposite direction. The start of the profile roughly resembles that of the original $\sigma = 3.5$ Pa test, suggesting that the various mechanisms (particle rearrangement and stochastic bond breakages) responsible for the onset of flow are similar in both cases. However, instead of becoming immobilized, the sample subsequently enters a fluidlike regime (linear increase in the magnitude of strain with time) in the reverse direction. Therefore, the strain-induced strengthening presented above only occurs in the original shear direction, and regardless of its detailed origin [extensional chain formation, Fig. 3(a), or cluster densification, Fig. 3(b)], it is connected to, or possibly even stems from microstructural anisotropy in the deformed gel. As mentioned earlier, flow microscopy would provide an invaluable tool for better understanding the microstructural events that govern this behavior.

IV. CONCLUDING REMARKS

In conclusion, we have investigated the nonlinear rheology of dilute colloidal gels induced by depletion interactions. We report that these systems yield via a two-step mechanism with origins necessarily unique from those in dense gels and glasses. We propose that the first yield point stems from bond rotations and structural rearrangements that begin to unravel the tenuous gel backbone, while the second yield point corresponds to the rupture of interparticle bonds. Application of an intermediate shear stress between the two yield points can result in remarkable creep behavior highlighted by two-stage deformation and anisotropic strain-induced strengthening of the gel, which we attribute to the formation of extensional force chains in the shear field. Our results suggest important connections between soft pivot points, two-step yielding, and nonlinear shear-induced strengthening in dilute colloidal gels. The occurrence of two-step yielding in dilute gels directly counters what has been previously suggested in the literature. We interpret this as evidence that much is still unknown about the nonlinear rheology of colloidal gels, and that further studies that capture the microstructural origins of these distinct yielding transitions are warranted.

ACKNOWLEDGMENTS

Financial support for this study was provided to A.M. by the National Science Foundation. We thank an anonymous reviewer for suggesting cluster densification as a possible mechanism of flow arrest.

[1] R. G. Larson, *The Structure and Rheology of Complex Fluids* (Oxford University Press, New York, 1998).
[2] E. Dickinson, *An Introduction to Food Colloids* (Oxford University Press, Oxford, 1992).
[3] J. Eisenlauer and E. Killmann, J. Colloid Interface Sci. **74**, 108 (1980).
[4] A. S. Kim and R. Yuan, J. Membr. Sci. **286**, 260 (2006).
[5] J. A. Lewis, J. Am. Ceram. Soc. **83**, 2341 (2000).

[6] J. E. Smay, J. Cesarano, and J. A. Lewis, Langmuir **18**, 5429 (2002).
[7] M. C. George, A. Mohraz, M. Piech, N. S. Bell, J. A. Lewis, and P. V. Braun, Adv. Mater. **21**, 66 (2009).
[8] J. Smay, G. Gratson, R. Shepherd, J. Cesarano, and J. Lewis, Adv. Mater. **14**, 1279 (2002).
[9] M. E. Fagan and C. F. Zukoski, J. Rheol. **41**, 373 (1997).
[10] R. Buscall, P. Mills, R. Stewart, D. Sutton, L. White, and G. Yates, J. Non-Newtonian Fluid Mech. **24**, 183 (1987).
[11] C. J. Rueb and C. F. Zukoski, J. Rheol. **41**, 197 (1997).
[12] W. H. Shih, W. Y. Shih, S. I. Kim, J. Liu, and I. A. Aksay, Phys. Rev. A **42**, 4772 (1990).
[13] S. Ramakrishnan and C. F. Zukoski, Langmuir **22**, 7833 (2006).
[14] X. Cao, H. Cummins, and J. Morris, Soft Matter **6**, 5425 (2010).
[15] A. T. J. M. Woutersen and C. G. de Kruif, J. Chem. Phys. **94**, 5739 (1991).
[16] R. de Rooij, A. A. Potanin, D. van den Ende, and J. Mellema, J. Chem. Phys. **99**, 9213 (1993).
[17] R. Buscall, J. I. McGowan, and A. J. Morton-Jones, J. Rheol. **37**, 621 (1993).
[18] M. Kogan and M. J. Solomon, Langmuir **26**, 1207 (2010).
[19] N. Koumakis and G. Petekidis, Soft Matter **7**, 2456 (2011).
[20] K. N. Pham, G. Petekidis, D. Vlassopoulos, S. U. Egelhaaf, W. C. K. Poon, and P. N. Pusey, J. Rheol. **52**, 649 (2008).
[21] J. Sprakel, S. B. Lindström, T. E. Kodger, and D. A. Weitz, Phys. Rev. Lett. **106**, 248303 (2011).
[22] M. Laurati, S. U. Egelhaaf, and G. Petekidis, J. Rheol. **55**, 673 (2011).
[23] K. N. Pham, G. Petekidis, D. Vlassopoulos, S. U. Egelhaaf, P. N. Pusey, and W. C. K. Poon, Europhys. Lett. **75**, 624 (2006).
[24] R. C. Kramb and C. F. Zukoski, J. Phys.: Condens. Matter **23**, 035102 (2011).
[25] G. Petekidis, D. Vlassopoulos, and P. N. Pusey, J. Phys.: Condens. Matter **16**, S3955 (2004).
[26] E. R. Weeks and D. A. Weitz, Phys. Rev. Lett. **89**, 095704 (2002).
[27] P. Coussot, H. Tabuteau, X. Chateau, L. Tocquer, and G. Ovarlez, J. Rheol. **50**, 975 (2006).
[28] A. A. Potanin, R. D. Rooij, D. V. den Ende, and J. Mellema, J. Chem. Phys. **102**, 5845 (1995).
[29] A. Mohraz and M. J. Solomon, J. Rheol. **49**, 657 (2005).
[30] B. Rajaram and A. Mohraz, Soft Matter **6**, 2246 (2010).
[31] J. P. Pantina and E. M. Furst, Phys. Rev. Lett. **94**, 138301 (2005).
[32] E. M. Furst and J. P. Pantina, Phys. Rev. E **75**, 050402 (2007).
[33] A. I. Campbell and P. Bartlett, J. Colloid Interface Sci. **256**, 325 (2002).
[34] M. T. Elsesser and A. D. Hollingsworth, Langmuir **26**, 17989 (2010).
[35] M. M. van Schooneveld, V. W. A. de Villeneuve, R. P. A. Dullens, D. G. A. L. Aarts, M. E. Leunissen, and W. K. Kegel, J. Phys. Chem. B **113**, 4560 (2009).
[36] G. E. Fernandes, D. J. Beltran-Villegas, and M. A. Bevan, Langmuir **24**, 10776 (2008).
[37] See Supplemental Material at http://link.aps.org/supplemental/10.1103/PhysRevE.85.041403 for linear viscoelasticity measurements and additional creep and recovery tests.
[38] G. Ovarlez and X. Chateau, Phys. Rev. E **77**, 061403 (2008).
[39] A. D. Dinsmore and D. A. Weitz, J. Phys.: Condens. Matter **14**, 7581 (2002).
[40] M. Carpineti and M. Giglio, Phys. Rev. Lett. **70**, 3828 (1993).
[41] B. Rajaram and A. Mohraz, Phys. Rev. E **84**, 011405 (2011).
[42] A. Zaccone, D. Gentili, H. Wu, M. Morbidelli, and E. Del Gado, Phys. Rev. Lett. **106**, 138301 (2011).
[43] C. P. Royall, S. R. Williams, T. Ohtsuka, and H. Tanaka, Nature Mater. **7**, 556 (2008).